ISSN 1870-4069

An Elitism Based Genetic Algorithm for Welding Sequence Optimization to Reduce Deformation

Jesus Romero-Hdz[1], Sinai Aranda[2], Gengis Toledo-Ramirez[1], Jose Segura[1], Baidya Saha[3]

[1] Centro de Ingeniería y Desarrollo Industrial (CIDESI), Mexico

[2] Universidad Tecnológica de Nayarit (UTN), Mexico

[3] Centro de Investigación en Matemáticas (CIMAT), Mexico

{jaromero,gengis.toledo,jose.segura}@cidesi.edu.mx,
sinaivoz@gmail.com, baidya.saha@cimat.mx

Abstract. This paper reports the development and implementation of a Genetic Algorithm (GA) based on welding sequence optimization in which a structural deformation is computed as a fitness function. Moreover, a thermo-mechanical finite element analysis (FEA) was used to predict deformation. Elitism selection approach has been used to ensure that the three best individuals are copied over once into the next generation to expedite convergence by preserving qualified individuals having the potential of generating optimal solution. We exploited a sequential string searching algorithm into single point crossover method to avoid the repetition of single beads into the sequence. We utilized a bit string mutation algorithm by changing the direction of the welding from one bead chosen randomly from the sequence to avoid the repetition of the weld seams in the sequence. We computed the minimum number of iterations required for elitism GA based on the general Markov chain model of GA. Welding simulation experiments were conducted on a typical widely used mounting bracket which has eight seams using well-known software Simufact®. Simulation results were validated through a experiment and a fair amount of agreement was achieved in terms of deformation pattern. This algorithm allowed the reduction up to ($\sim$80%). Finally elitism-based GA effectively reduces the computational complexity over exhaustive search.

Keywords: Genetic algorithm, welding deformation, AI application, welding sequence, welding optimization.

1 Introduction

Welding is the most common metal joining process [7]. It is widely used in various industries such as automotive, shipbuilding, aerospace, construction, gas and oil trucking, nuclear, pressure vessels, heavy and earth-moving equipment [18,11]. Nevertheless, welding deformation plays a negative role in the process having high impacts in several ways, such as constraints in the design phase, reworks, quality cost and overall capital expenditure. Welding sequence optimization significantly reduces welding deformation. The conventional approach is to select the best sequence by experience using a simplified design of experiments which often does not offer an optimal sequence [15]. Welding deformation can be numerically computed through finite element analysis (FEA) where thermo-mechanical models are commonly used. FEA offers reasonable solutions for various welding conditions and geometric configurations. However, under certain circumstances it can be computationally very expensive and time consuming.

The optimal welding sequence is olnly guaranteed using a full factorial design procedure. In this sense, the total number of welding configurations (N) are computed by $N = n^r \times r!$, where n and r are the number of welding directions and beads (seams) respectively. These possible configurations grows exponentially with the number of welding segments. For example, in this research we have used eight weld seams and two welding directions, hence the number of welding configurations for exhaustive search is 10,321,920. Considering a practical scenario, a complex weldment like an aero-engine assembly might have between 52 and 64 weld segments [12]. Therefore, full factorial design is often practically infeasible even using FEA.

In this paper, we implement a GA for welding sequence optimization. We make the following technical contributions. First, deformation based GA significantly reduces the computational complexity over extensive search. In the study case proposed in this paper, we achieved the optimal solution through GA after executing 72 welding configurations. In addition, this is the minimum number of iterations necessary to find the pseudo-optimal solution, which was found based on the general Markov chain model of GA. Second, we exploited a fitness function consisting of the inverse of the maximum structural deformation for welding sequence optimization. Third, we facilitated the convergence of the GA through the elitism selection approach in which we copied the three best individuals into the next generation and preserved the qualified individuals which possess high probability of providing an optimal solution. Fourth, we adjusted the single point crossover method for welding sequence optimization to avoid the repetition of single beads in the welding sequence by blending a sequential string searching algorithm into the single point crossover method. Finally, we implemented the bit string mutation algorithm by altering only the direction of welding instead of changing the bead itself to avoid seam repetition. One bead is selected randomly.

Gas Metal Arc Welding (GMAW) simulation experiments were conducted through the well-known simulation software Simufact Welding®. The average execution time for each welding configuration is 30 minutes using a workstation with two Intel® Xeon® @2.40 GHz, 48G GB of RAM and 4 GB of dedicated video memory. The study case in this paper is a mounting bracket which is widely used in telescopic jib [5] and automotive industries [21,10] among others. Simulation results were validated through real welding experiment. There exists a high agreement among the results of simulation and experiment in terms deformation pattern. Experimental results demonstrate that best welding sequence can reduce significant amount of structural deformation ($\sim$80%) over worst sequence.

The organization of the paper is as follows. Section 2 presents literature review. Section 3 discusses the thermal and mechanical analysis of finite element based welding simulation method. Proposed deformation based GA for welding sequence optimization and its convergence analysis is presented in Section 4. Results are demonstrated in Section 5. Section 6 concludes this work. Relevant references are listed at the end of the paper.

2 Literature Review

Concerning the welding deformation problem this section overviews five relevant papers published in the last decade. Chapple *et al.* [4] have developed a GA approach for welding distortion optimization from two perspectives: (i) weld removal optimization and (ii) a combination of weld removal and welding sequence optimization. They proposed a fitness function in terms of total distortion in a critical region as shown in Equation 1. However, constrains on stress and stiffness were added in weld removal optimization to prevent removing many weld seams. A simplified FEA was used for fitness function evaluation:

$$\begin{gathered} F = Min(Max(D_i)) \text{ if } S_i > T, \\ i = 1,2,3...N \qquad i \in R_c, \end{gathered} \tag{1}$$

where D_i is the total deformation for all nodes i in the critical region R_c, S_i is the stiffness of the structure and T is the minimum stiffness defined value. Total deformation is computed by the following equation:

$$D_i = \sqrt{{d_{x_i}}^2 + {d_{y_i}}^2 + {d_{z_i}}^2}, \tag{2}$$

where d_{x_i}, d_{y_i}, and d_{z_i} are the deformations of node i along x, y, and z axis respectively.

Islam *et al.* [11] have implemented GA in order to minimize the distortion in welded structures. They exploited a fitness function in terms of the maximum distortion on the overall structure. They have a conditional that includes a penalty term which is proportional to the number of nodes on the weld seam that have temperature less than melting value Equation 3. The penalty term determines upper and lower bounds for welding process parameters such as current, voltage and speed. They also defined six variables for possible welding direction. A thermo-mechanical FEA was carried out on a specimen as well as an automotive part. Experimental tryouts were done on a specimen using GMAW process:

$$F = \begin{Bmatrix} g & \text{IF} & Q = 0 \\ g + M_1 & \text{IF} & Q > 0 \end{Bmatrix}, \tag{3}$$

where

$$g = Min(Max(D_i)), \tag{4}$$

$$M_1 = 100Q. \tag{5}$$

D_i is the total deformation given by Equation 2, Q are the number of nodes in the weld seam that are below the melting point; M_1 is a penalty term that is proportional to Q.

Mohammed *et al.* [19] present an optimization procedure where GA and FEA minimize the welding induced distortion. The fitness function (Equation 6) used in their work is in terms of displacements along Z geometrical axis. This fitness function was developed for the simplified model of an aero-engine part where the distortion on Z axis dominates the other ones:

$$\begin{gathered} \text{Min } F = \text{Max}(|(d_z)_i|), \\ i = 1,2,3,...,N, \end{gathered} \tag{6}$$

where d_z is the deformation on z axis and N the total amount of nodes.

Liao [16] presents an implementation of GA for searching the optimal weld pattern in a spot welding process. The proposed fitness function is computed in two ways, first, in a deterministic mode which means the future states depend from the previous ones. Second, in a stochastic mode where the future states do not depend from the previous ones. FEA was used to compute the fitness function. The fitness function for the deterministic mode is shown in Equation 7:

$$\begin{gathered} F = \sum_{i=1}^{n} w_{1i}(D_i)^2, \\ i = 1,2,3,...,N, \end{gathered} \tag{7}$$

where w_{1i} is a weight factor that determines the importance of each node; D_i is the total deformation on all the nodes N. The fitness function for the stochastic mode is shown in equation 8:

$$\begin{gathered} F = \sum_{i=1}^{n} w_{1i}(U_i)^2 + \mathrm{w}_{2i}(\mathrm{V}_i), \\ i = 1,2,3,...,N, \end{gathered} \tag{8}$$

where w_{1i} and w_{2i} are weights, U_i is the average deformation on every single node and V_i is the variance of the deformation.

Xie and Hsieh [22] have implemented GA for finding a combined clamping and welding sequence. A multi-objective fitness function is taken into account to minimize cycle time (gun travel path) and assembly deformation as shown in Equation 9. FEA was used to evaluate the fitness function on automotive parts joined by spot welding process:

$$\begin{gathered} \text{Min } F = w_1 \frac{D_i}{D_{0i}} + w_2 \frac{C}{C_0}, \\ i = 1,2,3,...,N, \end{gathered} \tag{9}$$

where w_1 and w_2 are weights that define the importance of each sub-function; D_i is the total deformation on all nodes for the actual generation. D_{0i} is the total deformation on all nodes for the initial generation; C is the cycle time for the actual generation and C_0 is the cycle time for the initial generation. Notice that $\frac{D_i}{D_{0i}}$ and $\frac{C}{C_0}$ are considered as normalized functions because the units of deformation and cycle time are different.

3 Welding Simulation Framework

In order to present our approach we overview the welding simulation framework. This is important because the fitness function is computed using FEA.

3.1 Thermal Analysis

Weld process modeling (WPM) is quite complex task because of the physics of heat generation, specially for fusion processess like GMAW. The fundamental principle that defines the heat source is the law of conservation of energy [7]. Typically, the complexity of heat generation physics in the weld puddle is simplified by using a heat input model. The classical approach in Computational Welding Mechanics (CWM) is to ignore fluid flow and use a heat input model where heat distribution is prescribed. The given heat input replaces the details of the heat generation process and focus on larger scales. Moreover, the modeling of fluid flow and pertaining convective heat transfer may be integrated with a CWM model. The most common used model for fusion welding processes is the well-known Goldak double ellipsoidal heat distribution [7]. This heat input model combines two ellipsoidal heat sources to achieve the expected steeper temperature gradient in front of the heat source and a less steep gradient at the trailing edge of molten pool. This two heat sources are defined as follow:
Front heat distribution:

$$Q(x',y',z',t) = \frac{6\sqrt{3}f_f Q_w}{\pi\sqrt{\pi}abc_f} e^{\left(\frac{-3x'^2}{a^2}\right)} e^{\left(\frac{-3y'^2}{b^2}\right)} e^{\left(\frac{-3z'^2}{C_f{}^2}\right)}. \tag{10}$$

Rear heat distribution:

$$Q(x',y',z',t) = \frac{6\sqrt{3}f_r Q_w}{\pi\sqrt{\pi}abc_r} e^{\left(\frac{-3x'^2}{a^2}\right)} e^{\left(\frac{-3y'^2}{b^2}\right)} e^{\left(\frac{-3z'^2}{C_r{}^2}\right)}, \tag{11}$$

where f_f is the fraction factor of heat deposited in the front part, f_r is the fraction factor of heat deposited in the rear part. Those factors must satisfy the relation $f_f + f_r = 2$. a is the width, b is depth, c_f is the length of the front ellipsoid and c_r is the length of the rear ellipsoid Figure 1.

These parameters are physically related to the shape of the weld puddle. Width and depth are commonly taken from the cross section, the authors recommend to use a half of parameter a for the front fraction and two times a for the rear fraction. The heat available from the heat source is defined by:

$$Q_w = \eta I E, \tag{12}$$

where η is the heat source efficiency, I is the current (A) , E is the voltage (V).

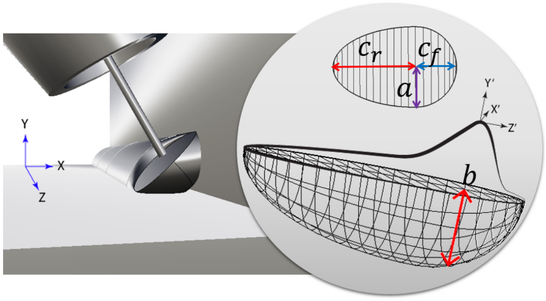

Fig. 1. Goldak double ellipsoidal model.

Thus the heat input model in CWM must be calibrated with respect to experiments. Therefore, the classical CWM models have some limitations in their predictive power to solve different engineering problems. For example, they cannot prescribe what penetration a given welding procedure will give. The appropriate procedure to determine the heat input model is therefore important in CWM [17].

FEA software solves this time dependent system of partial differential equations on a domain defined by the mesh used in FEA. The domain is dynamic because of it changes with each time step as filler metal is added to the weld pass. The initial condition is often assumed to be the ambient temperature, but the domain can be initialized to any initial temperature field. The heating effect of the arc is often modeled by a double ellipsoid power density distribution that approximates the weld pool as measured from macro-graphs of the cross-section of several weld passes. A convection boundary condition $q = h(T - T_{amb})$ with convection coefficient h and ambient temperature T_m usually is applied to external surfaces. The FEM formulation of the heat equation leads to a set of ordinary differential equations that are integrated in time using a backward Euler integration scheme.

3.2 Mechanical Analysis

The temperature history from the thermal analysis is used as a series of loads in the structural analysis. In this phase, the temperature history from the thermal cycle of each node is taken as an input and it is used as a node load with temperature dependent material properties. The mesh for the mechanical analysis was also used for the thermal analysis where each increment of weld deposition corresponded to one load step. The total strain ε^{total} (assuming negligible contribution from solid state phase transformation) can be decomposed into three components as follows: $\varepsilon^{total} = \varepsilon^e + \varepsilon^p + \varepsilon^{th}$, where $\varepsilon^e, \varepsilon^p$, and ε^{th} represent elastic, plastic and thermal strain respectively. In the welding process, changes in stress caused by deformation are assumed to travel slowly compared to the speed of sound. So, at any instant, an observed group of material particles is approximately in static equilibrium, i.e., inertial forces are neglected. In rate independent plasticity, viscosity is zero and viscous forces are zero. In either the Lagrangian or the Eulerian reference frame, the partial differential equation of equilibrium is, at any

moment given by the conservation of momentum equation that is mentioned below [6]:
Conservation of Momentum Equation

$$\begin{aligned} \nabla\sigma + f &= 0, \\ \sigma &= D\varepsilon, \\ \varepsilon &= (\nabla u + (\nabla u)^T + (\nabla u)^T \nabla u)/2, \end{aligned} \tag{13}$$

where $\nabla, \sigma, f, D, \varepsilon$ and u represent partial differential, Cauchy stress, total body force, temperature dependent material property (elastic matrix relevant to the modulus of elasticity and Poisson's ratio), the Green-Lagrange strain and displacement vector respectively. ∇u represents the displacement gradient. The mechanical model is based on the solution of three partial differential equations of force equilibrium illustrated in Equation 13. In the FEM formulation, Equation 13 is transformed and integrated over the physical domain, or a reference domain with a unique mapping to the physical domain [7]. FEA software solves this partial differential equation for a viscothermo-elasto-plastic stress-strain relationship. The initial state often is assumed to be stress free. Dirichlet boundary conditions constrain the rigid body modes. The system is solved using a time marching scheme with time step lengths of approximately 0.1 second during welding and 5 second during cooling phase.

4 Welding sequence optimization framework

GA emulate natural selection of a set of individuals in order to search the best solution to a problem [8]. The genetic configuration of each individual is a possible solution. The algorithm starts with an initial population and those are submitted to an evolutionary process in such way that the best adapted individuals will continue to reproduce among them and over several generations the best adapted stands out. We tailor the GA for the welding sequence optimization: selection, cross-over and mutation to avoid the repetition of single bead.

4.1 String Representation of Welding Sequence

Being Q a welding application consisting of a set of welding beads and S a set of all possible sequences of Q, each sequence $s \in S$ represents a possible sequence which minimizes the overall structure deformation. Each sequence has N weld seams, here called genes $s = \{x^1, x^2, x^3, \ldots, x^N\}$, these are a combination of real numbers $\forall n = 1, 2, 3, ,..., N$. In this approach every seam can be welded in two directions, so it can be represented by a positive sign $if \circlearrowleft or \uparrow or \leftarrow$ or with a negative sign $if \circlearrowright or \downarrow or \rightarrow$.

4.2 Initialization of Welding Sequence

The algorithm starts with an initial population $P = \{s_j\}$, where elements of the set of sequences are called "individuals" $j = 1, 2, 3, ..., J$. Their genes are generated randomly and special considerations are taken in order to avoid repeated seam in the same welding sequence.

4.3 Deformation Based Fitness Value

Within the scope of natural selection, the individual eligibility is regarded as the degree of adaptability. In this paper the fitness function (Equation 14) returns a real number (maximum deformation) $f\left(s_{j=1}^{J}\right) \Rightarrow \mathbb{R}$ that measures the adaptability of each sequence. Final deformation is computed by FEA:

$$f(s_j) = 1/(Max(D_i) + \varepsilon), \tag{14}$$

where D_i is the total deformation on all nodes defined by:

$$D_i = \sqrt{{d_{x_i}}^2 + {d_{y_i}}^2 + {d_{z_i}}^2}, \tag{15}$$

$$i = 1, 2, 3, \ldots, N,$$

d_{x_i}, d_{y_i}, and d_{z_i} are deformations at the node i along x, y, and z axis respectively. ε is a very small number which was used to offer continuity to the fitness function when the value of the maximum deformation is zero.

4.4 Welding Sequence Selection Algorithm

Selection is an important sub-routine where individuals are chosen from the actual population for later procreation. Good selection algorithm expedites the convergence of the welding sequence. As a selection procedure, we first implemented a truncation procedure where the population is sorted by ascending fitness values, then a proportion μ of the individuals are taken based on fitness value. The proportion μ is computed by the fraction of the individual fitness value to the sum of the fitness values of all the samples as shown in Fig. 2.

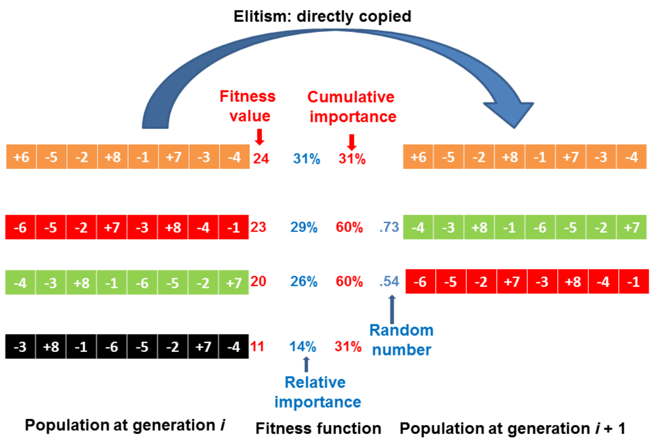

Fig. 2. Selection process using an elitism function.

4.5 Crossover for Generating New Welding Sequences

Crossover is analogous to reproduction, new individuals are created from the selected parents. Each couple of selected individuals s_1 and s_2 exchange their genes and make two new individuals, $s'_1 = s_1 \times s_2$ and $s'_2 = s_2 \times s_1$. Several methods for crossover are reported in literature such as arithmetic, heuristic, single or multi-point, uniform, cycle, partially mapped and order [13,9]. In this paper we implemented a single point crossover as demonstrated in Fig. 3 where a random number defines the cut point $a \in [1,N]$. Later, the descendants are defined by Equations 16 y 17 respectively:

$$s'_1 = \left\{[x_1^1, \ldots x_1^a], [x_2^{a+1}, \ldots x_2^N]\right\}, \tag{16}$$

$$s'_2 = \left\{[x_2^1, \ldots x_2^a], [x_1^{a+1}, \ldots x_1^N]\right\}. \tag{17}$$

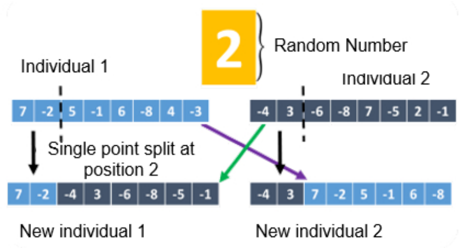

Fig. 3. Single point crossover process.

To avoid the repetition of the weld seam in the same welding sequence during crossover we implement a REPEATED STRING VALIDATION algorithm, the pseudo-code of which is illustrated below.

function REPEATED STRING VALIDATION
  random number $a \in [1, N-1]$;
  $s'_1 = \{x_1^1, \ldots x_1^a\}$;
  $s'_2 = \{x_2^{a+1}, \ldots x_2^N\}$;
  for $i = 1 : N$ **do**
    if $\Pi(\sqrt{s'_1 .* s'_1}) \neq \sqrt{s_2(i)' .* s_2(i)'}$ **then**
      $s'_1 = \{[s'_1] \cup s_2(i)'\}$;
    end if
    if $\Pi(\sqrt{s'_2 .* s'_2}) \neq \sqrt{s_1(i)' .* s_1(i)'}$ **then**
      $s'_2 = \{[s'_2] \cup s_1(i)'\}$;
    end if
  end for
end function

4.6 Mutation for Generating New Welding Sequences

Mutation alters one or more genes in the individual from its actual configuration. It occurs during the evolution in a very low incidence according to a defined mutation probability. Some of the operators found in literature are bit string, delta, invert and swap [20,1,14]. In our approach, we have used a bit string operator in order to change only the direction of welding, rather than the welding seam itself to avoid the repetition of the weld seam (Fig. 4).

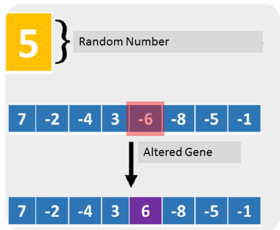

Fig. 4. Mutation using a bit string operator.

4.7 Elitism Based Welding Sequence Selection Algorithm

The *Elitism* function is a practical variant that ensures that the best individual in the current population $s_{best} \in P_t$ and current generation t is carry over to the next generation P_{t+1} (Fig. 2). Elitist based selection algorithm guarantees that the convergence obtained by the GA will follow monotone decreasing behavior over generations, $[s_{best} \in P_t] \rightarrow P_{t+1}$.

4.8 Pseudo-code and Flowchart of the Proposed Iterative GA for the Welding Sequence Optimization

This GA function is a repetitive process where the population is going to be changing over generations: $P_t = (s_1(t),\ s_2(t), \ldots s_J(t)) \in S$. The pseudo-code for the proposed GA based welding sequence optimization is given below.

function GA($Min\ D : Q$)
Input: $P_0 = (s_1(t),\ s_2(t), \ldots,\ s_J(t)) \in S$
Output: s_{best}, the best sequence that shows minimum deformation.

$t \leftarrow 0$;
initialize $P_t \in S$;
evaluate $f\left(s_{j=1}^{J}\right)$;
while !terminating condition **do**
$t++$;
Select P_t from P_{t-1} based on the relative importance of the value of the individual fitness function $f(s_j)$; /* Priority given to the welding sequences based on less deformation */
crossover $P_t \leftarrow P_t$; /* String searching based single point crossover */

mutation $P_t \leftarrow P_t$; /* Change the direction of the welding of one seam */
evaluate $f\left(s^J_{j=1}\right)$;
elitism $P_t \leftarrow s_{best}$ from P_t; /* Elitism based selection approach */
end while
return s_{best} from P_t.
end function

In Figure 5 we present a flowchart where we describe at detail our GA based welding sequence optimization approach.

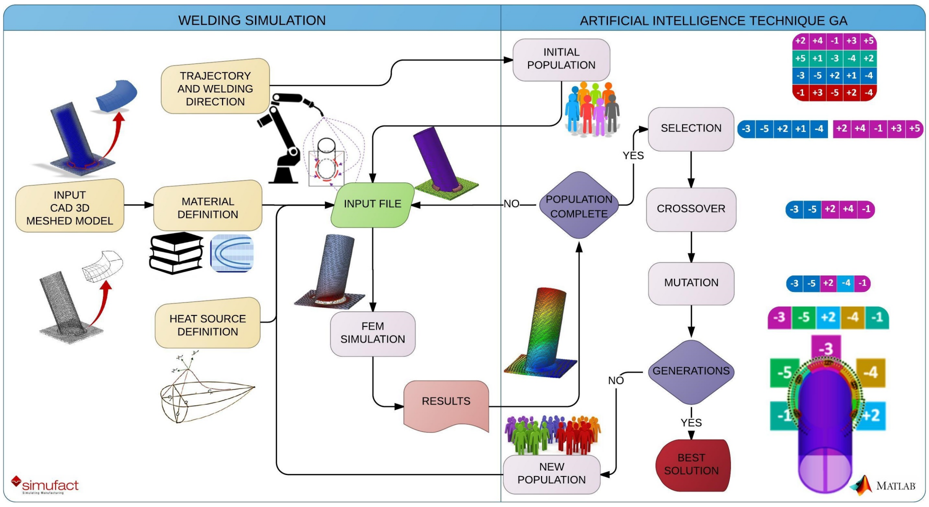

Fig. 5. GA based welding sequence optimization approach.

4.9 Convergence Analysis of the GA

For a general Markov chain model of GA with elitism, an upper bound for the number of iterations t is required to generate a population S^+ consisting of minimal solutions has been generated with probability $\alpha \in (0,1)$ [2,3], is given by

$$t \geq \lceil \frac{ln(1-\alpha)}{nln(1-min\{\mu^l,(1-\mu)^l\})} \rceil, \tag{18}$$

where l is the length of the chains that represent the individual, n is the population size and $\mu \in (0,1)$ is the mutation rate. $\lceil x \rceil$ is the smallest integer greater than or equal to x. Equation 18 reaches to minimum when $\mu = 0.5$. For faster convergence, in our experiment we chose the value of $\mu = 0.5$ since the thermo-mechanical finite element analysis based welding simulation model is computationally very expensive.

5 Experimental Results

The organization of this section is as follows. First we introduce the study case. Second, we list the parameters used for this study. Third, we present convergence analysis of proposed GA. Fourth, we describe the effects of welding sequence on welding process optimization. Fifth, we show experimental validation of the simulation results. And finally, we show a comparative study: Simulation vs real experiment.

5.1 Study Case

We chose a study case of welding a mounting bracket shown in Fig. 6 and 7 which is typically used in telescopic jib [5], automotive industries [21], and cars [10]. We conducted a simulation experiment of GMAW process using popular FEA software. [11]. We implemented a GA algorithm for choosing the best welding sequence having minimum deformation and we demonstrated the effects of welding sequence on the weld quality (structural deformation) by analyzing the structural deformation caused by welding of the four sequences (the best two and worst two found by GA). We used the same parameters for all the sequences (Table 1). We divided the welding bead into eight segments as shown in Fig. 7. In Fig. 6 we show geometries of different mounting brackets that can be found frequently in heavy equipment, vehicles, ships. Fig. 7 illustrates the engineering drawing with all specifications of the mounting bracket used in this experiment.

Fig. 6. Different mounting brackets available in the market as an example of welded parts.

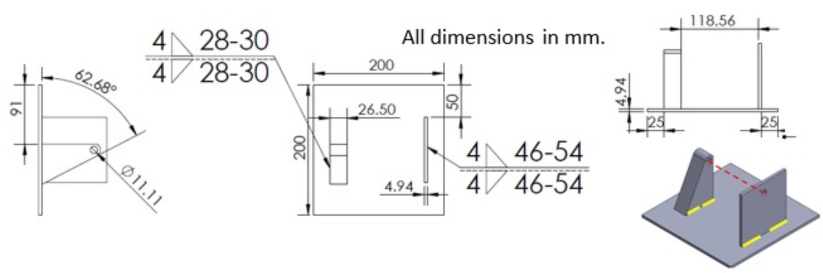

Fig. 7. Engineering drawing of the study case with 8 seams.

5.2 Parameters Used for this Study

Table 1 shows the GA parameters used in the simulation experiment. We considered 12 generations to converge the GA algorithm, initial population size as 6, crossover probability as 50%. We copy the three best candidates of the current generation to the next generation using elitism selection mechanism. We implemented single point crossover method for new sample reproduction. We also implemented single bit string mutation operator and changed the welding direction of a randomly selected welding seam instead of welding seam itself to avoid the repetition of the welding seam in the sequence.

Table 1. GA parameters for welding sequence optimization.

Parameter	Value
Initial population size	6
Generations	12
Elitism candidates	3
Crossover %	50%
Mutation operator	bit string
Crossover operator	single point
Qty of seams	8
Possible welding directions	2

We have validated the result of the simulation experiment. Since conducting the real welding experiment is costly, we have conducted the real experiment for only the best sequence found by the GA. Fig. 8 illustrates the flowchart of the real experiment.

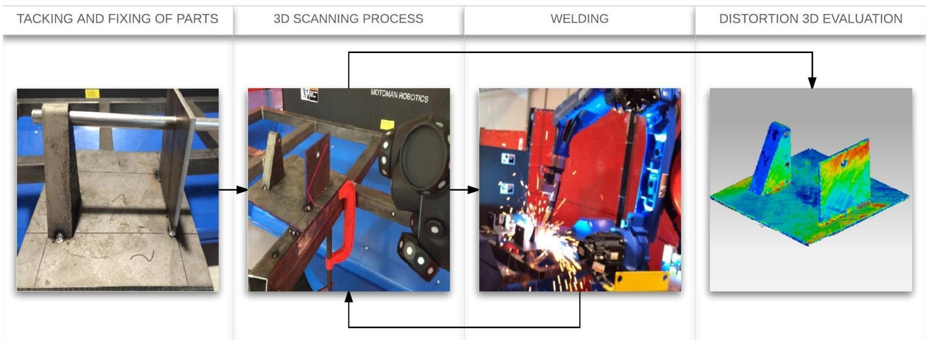

Fig. 8. Flowchart of the real experiment.

5.3 FEA Results and Convergence Analysis of the Proposed GA

The best, second best, worst and second worst sequences are $(+6, +5, -1, +8, -2, -3, +4, -7)$, $(+6, +5, -1, -8, -2, -3, +4, +7)$, $(-3, +4, -7, +6, +5, -1, +8, -2)$ and $(-3, +4, -7, +6, +5$

$, -1, -8, -2)$ respectively (Fig. 9). Their maximum structural deformation values are $0.55mm., 0.57mm., 2.43mm.$, and $2.42mm.$ respectively (Fig. 10). We carried out the GA experiment for twelve generations and we conducted the convergence analysis that is shown in Fig. 11. Fig. 11(a) shows the behavior of the individual in terms of deformation over generations for four sequences (best, second best, worst and second worst). Elitism based selection method expedites the convergence of the GA. Fig. 11(b) shows the monotonically decreasing values of the deformation over twelve generations.

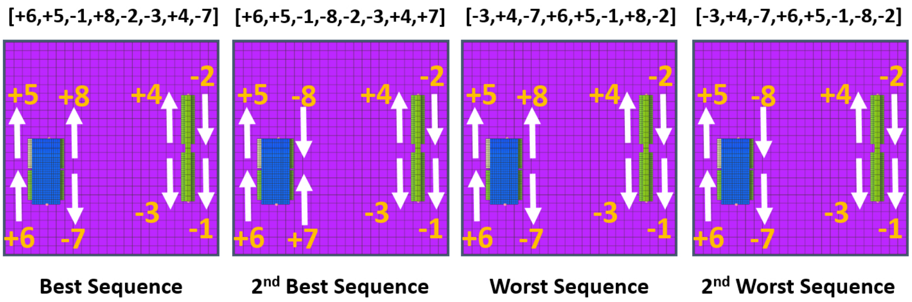

Fig. 9. Best, second best, worst and second worst sequences configuration.

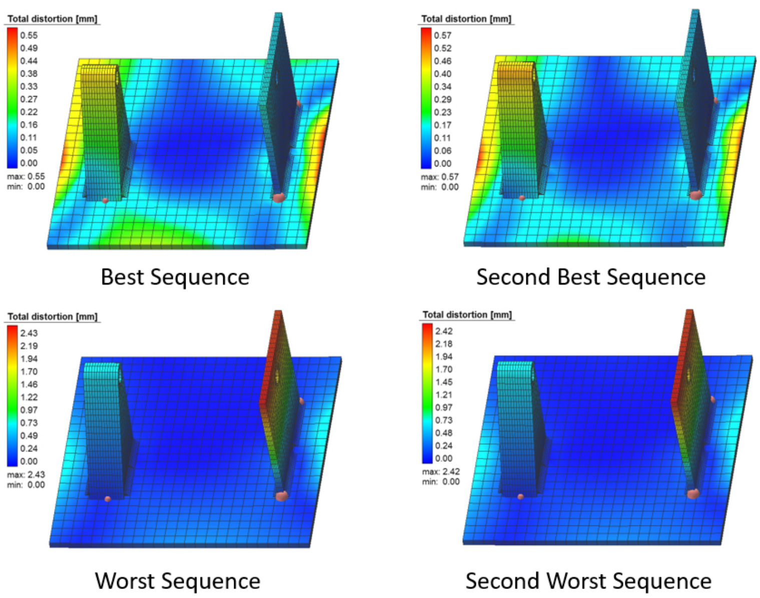

Fig. 10. Deformation pattern of best, second best, worst and second worst sequences.

To compute the minimum number of iterations necessary to ensure finding an optimal solution for GA with a prescribed probability $\alpha = 0.96$, mutation rate $\mu = 0.5$, number of bits required to represent an individual $l = 8$, number of individual $n = 72$ in equation 18, we get $t \geq \lceil 11.42 \rceil = 12$. We conduct the GA up to twelve iterations since the computational complexity of the finite element based thermo-mechanical welding simulation approach is computationally very expensive.

(a) Deformation over generations

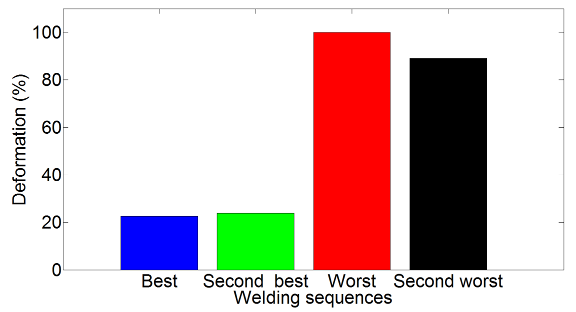

(b) Deformation Reduction

Fig. 11. Convergence analysis of proposed GA.

5.4 Effects of Welding Sequence on Welding Process Optimization

Normalized frequency of the deformation and effective stress values are shown in Fig. 12(a) and 12(b). Fig. 11(b) shows the deformation values of the four sequences in terms of the percentage. If we consider the deformation value of the worst sequence (red color bar in Fig. 11(b)) as 100%. Fig. 11(b) shows that best sequence (blue color bar) achieves $\sim$ 80% maximum structural deformation over worst sequence (red color bar). Fig. 11(b) also demonstrates that both best and second best sequences obtains substantial reduction of maximum structural deformation over worst and second worst sequences (red and black bars are much taller than blue and green bars). These results clearly demonstrates that welding sequence has significant effect on welding deformation.

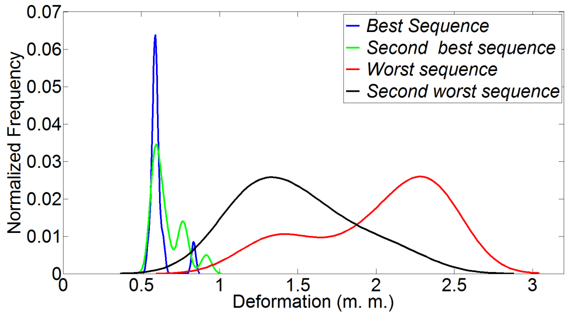

(a) Deformation

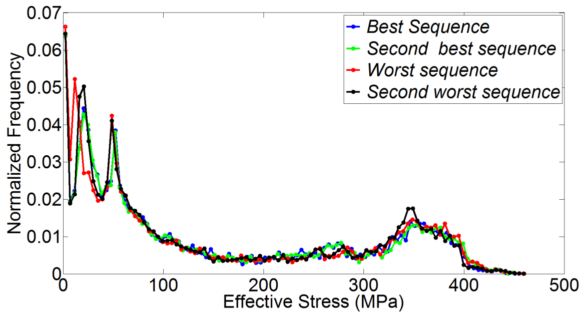

(b) Effective Stress

Fig. 12. Normal distribution of both experimental and simulation fitness values.

5.5 Experimental Validation of the Simulation Results

Thermal analysis was validated using thermocouples. In Figure. 13 we show the temperature curve acquired in one seam. It can be seen in the curve two peaks, the first one is the heat transferred from the other side of the plate over the time when the seam located there is being welded. On the other hand, the second peak is the temperature when the heat source reaches the thermocouple. It is observed that there is a good agreement between acquired temperatures of the welding simulation and thermocouples used in real experiment. Fig. 14 shows a three dimensional (3D) comparison between

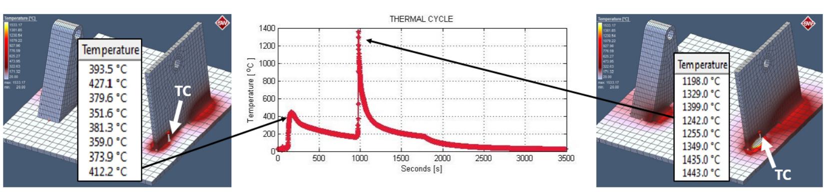

Fig. 13. Temperature acquired with thermocouples.

the structural deformation found in the real and simulation experiment for the best sequence $(+6, +5, -1, +8, -2, -3, +4, -7)$. For 3D visualization of real experiment, we used Geomagic Control® software with a Creaform® optical scanner and for simulation experiment, we used simufact® FEA software [11]. Fig. 14 demonstrates a good agreement between the structural deformation found in real and simulation experiment.

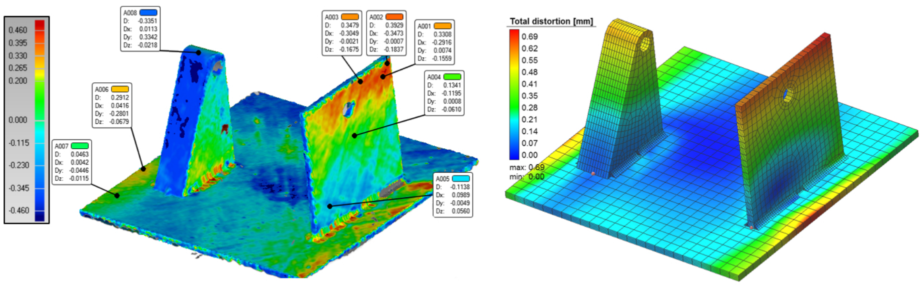

Fig. 14. Structural deformation comparison between real and simulated experiments.

5.6 Comparative Study: Simulation vs Real Experiment

Deformation values found in the experiment are below the predicted values found in the welding simulation. The difference between them is the cumulative error in the measurement process. 3D scanner has 0.085 mmm. of error, welding positioner has 0.1 mm of error and typically welding simulation is around 20% error (0.13 mm in this case). Lindgren [17] and Islam [11] showed that the main driving force in the welding simulation is heat generation process. If the simulation can predict the weld pool boundary correctly then the temperature field outside the region will also be correct. Therefore, the heat source model of the welding simulation was validated with respect to the weld macroetch test as shown in Fig. 15 and a fairly good agreement was achieved in terms of weld pool boundary shape and size. The red and yellow line illustrates the weld pool boundary of real and simulation experiment respectively.

6 Conclusion and Future Work

Structural deformation is an important parameter to measure the quality of the welded structures. Welding sequence plays an important role on welding deformation. In this paper, the inverse of the maximum structural deformation was exploited as the fitness function of a proposed GA algorithm for welding sequence optimization. GA was used to reduce significantly the search space of the exhaustive search. A finite element based thermo-mechanical analysis was used to compute the deformation. An elitism selection approach was implemented by copying the three best individuals into the

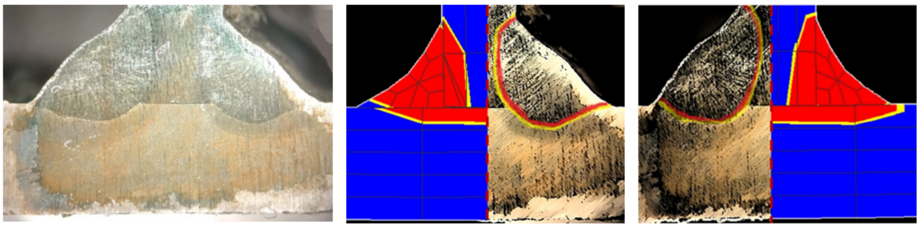

Fig. 15. Macroetch test and a comparison between real and simulation experiment.

next generation to expedite the convergence as well as not allowing to destroy the chromosomes which have high probability to offer optimal solution. We implemented a sequential string searching algorithm for a single point crossover method to avoid the repetition of single beads. We changed the welding direction of the bead, rather than the welding bead itself from the sequence into one bit string mutation algorithm to avoid the repetition of the weld seam. We conducted a simulation experiment on a mounting bracket which were widely used in vehicles and other applications. A experiment was conducted on eight weld seams. Results of simulations were validated through a real experiment by comparing the temperature recorded by thermocouples kept on different weld seams with the temperature computed by the thermo-mechanical FEA as well as comparing the structural deformation of real and simulation experiment. A reasonable agreement was achieved among the results of simulation and real experiment in terms of the temperature profile curve and the shape and size of the weld pool boundary. Elitism based GA algorithm discussed in this paper effectively reduces the computational complexity over extensive search with significant reduction of overall structure deformation. We computed and executed minimum number of iterations necessary for finding the optimal solution of the GA based on the general Markov chain model of GA.

The proposed research opens up different avenues for welding sequence optimization research. In the near future, we would like to develop a multi-objective GA to incorporate residual stress, temperature, robot time and robot path for welding sequence optimization. Information of the deformation after welding each seam in a sequence needs to be investigated for achieving better reduction of welding deformation.

Acknowledgments. The authors gratefully acknowledge the support provided by CONACYT (The National Council of Science and Technology) and CIDESI (Center for Engineering and Industrial Development) as well as their personnel that helped to realized this work.

References

1. Alexandrescu, A., Agavriloaei, I.: Determining the best mutation probabilities of a genetic algorithm for mapping tasks. The Bulletin of The Polytechnic Institute from Iaşi LVII (LXI)(Lxi), 10 (2011)

2. Aytug, H., J., K.G.: Stopping criteria for finite length genetic algorithms. INFORMS Journal on Computing 8(2), 183–191 (1996)
3. Aytug, H., J., K.G.: New stopping criterion for genetic algorithms. European Journal of Operational Research 126(3), 662–674 (2000), `http://www.sciencedirect.com/science/article/pii/S0377221799003215`
4. Chapple, A., Tahir, Z., Jardine, F.: Weld Distortion Optimisation using HyperStudy. In: The 8th UK Altair Technology Conference. pp. 1–13 (2013)
5. Derlukiewicz, D., Przybyek, G.: Chosen aspects of FEM strength analysis of telescopic jib mounted on mobile platform. Automation in Construction 17(3), 278–283 (2008), `http://www.sciencedirect.com/science/article/pii/S0926580507000714`
6. Goldak, J.: PVP2010-25770 Challenges in verification of cwm software to compute residual pp. 1–9 (2010)
7. Goldak, J.A., Akhlaghi, M.: Computational welding mechanics. Springer (2005), `http://www.worldcat.org/isbn/9780387232874`
8. Goldberg, D.E.: Genetic Algorithms in Search, Optimization and Machine Learning. Addison-Wesley Longman Publishing Co., Inc., Boston, MA, USA, 1st edn. (1989)
9. Hasançebi, O., Erbatur, F.: Evaluation of crossover techniques in genetic algorithm based optimum structural design. Computers & Structures 78(13), 435–448 (2000), `http://www.sciencedirect.com/science/article/pii/S0045794900000894`
10. Hussain, M.: Study of the dynamic behavior of a car body for mounting the rear axle 25, 782 (2016), `http://link.springer.com/10.1007/978-3-319-27276-4`
11. Islam, M., Buijk, A., Rais-Rohani, M., Motoyama, K.: Simulation-based numerical optimization of arc welding process for reduced distortion in welded structures. Finite Elements in Analysis and Design 84, 54–64 (jul 2014), `http://linkinghub.elsevier.com/retrieve/pii/S0168874X14000201`
12. Jackson, K., Darlington, R.: Advanced engineering methods for assessing welding distortion in aero-engine assemblies. IOP Conference Series: Materials Science and Engineering 26, 012018 (2011)
13. Kaya, Y., Uyar, M., Tekin, R.: A novel crossover operator for genetic algorithms: Ring crossover. CoRR abs/1105.0355 (2011), `http://dblp.uni-trier.de/db/journals/corr/corr1105.html#abs-1105-0355`
14. Koenig, A.: A Study of Mutation Methods for Evolutionary Algorithms. CS 447 - Advanced Topics in Artificial Intelligence pp. 1–8 (2002), `http://web.mst.edu/{~}tauritzd/courses/ec/fs2002/project/Koenig.pdf`
15. Kumar, D.A., Biswas, P., Mandal, N.R., Mahapatra, M.M.: A study on the effect of welding sequence in fabrication of large stiffened plate panels. Journal of Marine Science and Application 10(4), 429–436 (2011)
16. Liao, Y.G.: Optimal design of weld pattern in sheet metal assembly based on a genetic algorithm. International Journal of Advanced Manufacturing Technology 26(5-6), 512–516 (2005)
17. Lindgren, L.E.: Computational welding mechanics. In: Lindgren, L.E. (ed.) Computational Welding Mechanics, pp. 31–46. Woodhead Publishing Series in Welding and Other Joining Technologies, Woodhead Publishing (2007), `http://www.sciencedirect.com/science/article/pii/B9781845692216500045`
18. Masubuchi, K.: Analysis of Welded Structures, vol. 3. Pergamon Press Ltd. (1980)
19. Mohammed, M.B., Sun, W., Hyde, T.H.: Welding sequence optimization of plasma arc for welded thin structures. In: WIT Transactions on The Built Environment. vol. 125, pp. 231–242 (2012), `http://library.witpress.com/viewpaper.asp?pcode=OP12-020-1`
20. Soni, N., Kumar, T.: Study of Various Mutation Operators in Genetic Algorithms. International Journal of Computer Science and Information Technologies 5, 4519–4521 (2014)

21. Subbiah, S., Singh, O., Mohan, S.K., Jeyaraj, A.P.: Effect of muffler mounting bracket designs on durability. Engineering Failure Analysis 18(3), 1094–1107 (2011)
22. Xie, L.S., Hsieh, C.: Clamping and welding sequence optimization for minimizing cycle time and assembly deformation. International Journal of Materials & Product Technology 17(5/6), 389–399 (2002)